International Journal of Mechanical Sciences 52 (2010) 1767–1771

Contents lists available at ScienceDirect

International Journal of Mechanical Sciences

journal homepage: www.elsevier.com/locate/ijmecsci

Multi-displacement continuum model for discrete systems

Jia-Lin Tsai [a], Hsin-Haou Huang [b,*], C.T. Sun [b]

[a] Department of Mechanical Engineering, National Chiao Tung University, Hsin-Chu, Taiwan
[b] School of Aeronautics and Astronautics, Purdue University, W. Lafayette, IN 47907, USA

ARTICLE INFO

Article history:
Received 26 November 2009
Accepted 15 September 2010
Available online 19 September 2010

Keywords:
Lattice
Multi-displacement continuum theory
Wave propagation
Negative group velocity

ABSTRACT

A first-order multi-displacement microstructure continuum model is introduced to represent a discrete diatomic lattice system. This model is developed based on a two-term Taylor series expansion of the local displacement of the lattice. It is found that the multi-displacement continuum model obtained by keeping two terms in the Taylor series yields, in general, a better representation of the lattice system than the effective modulus model. However, this microstructure continuum model cannot characterize the negative group velocity of an optical mode of harmonic wave motion in the diatomic lattice. To capture the negative group velocity, a higher-order multi-displacement continuum model is necessary.

1. Introduction

Emerging nanotechnology has given rise to increased interest in modeling material behavior at the nanoscale. The analysis methods used for nanoscale includes, for example, ab initio, tight binding, and molecular dynamics. These methods are developed based on quantum mechanics with appropriate approximations. They can be accurate enough with expensive computation. Moreover these atomic approaches are mostly limited to small-scale problems due to the high cost of computation. One solution to resolve the problem is to rely on the equivalent continuum model. Such an approach yields great simplifications and has been widely adopted for modeling and analyzing discrete lattice structures [1,2]. By combining discrete atomic domains with continuum domains, a large-scale domain of interests can be analyzed. For instance, Kwon and Manthena [3] developed a homogenization technique to replace a discrete atomic domain by an equivalent continuum domain. An efficient finite-element analysis could therefore be performed for a large sized domain.

However, modern materials are becoming more and more complex. Many new materials are heterogeneous systems, which consist of multiple phases, each serving a different function. The conventional continuum approach may become inadequate in describing the response of solids with micro/nano-structures, when the characteristic length (or wavelength) of deformation becomes comparable to or smaller than the dimensions of the representative cell of the micro/nano-structure. An example is the wavelength-dependent wave velocity in composite materials. If a composite is modeled as a homogeneous elastic solid, then the bulk plane wave (longitudinal or shear) would propagate at a constant speed. In contrast, the exact solution based on the model that retains the identity of the microstructure (fiber, particle) indicates that the wave is dispersive meaning that the wave speed is not a constant, but is affected by wavelength.

The main reason for the aforementioned deficiency of the classical continuum model can be attributed to its inability to account for the local motion of the micro/nano-structure. A common way to solve this problem is to employ additional kinematic variables to describe the non-homogeneous local deformation in the microstructure of the solid. This approach leads to Cosserat type continuum models that are often attributed to the Cosserat brothers [4]. There are variations among these models which are often referred to as microstructure, micropolar, or micromorphic models [5–9]. Some authors have even attempted to use these extended continuum models to bridge continuum theory and molecular dynamics down to the atomic scale [10,11]. Common to all of the above models is that, in addition to the usual translational displacement vector to describe the average displacement, additional deformation kinematic variables or even multiple displacement vectors are introduced to describe the nonhomogeneous local deformation. Among the existing Cosserat continuum type models, most of them only present a general form of the governing equations; extensive experiments are required to determine numerous material constants associated with the models. On the other hand, the micro/nano-structure continuum models developed in [8,9,12–14] are based on the unit cell of the original material and all the material constants of the continuum models can be derived analytically from the micro/nano-structure. The governing equations are directly derived from the geometry and the mechanics of the micro or nano-structure in the unit cell.

In this study, we employ the multi-displacement approach to describe the local motions of microstructures. A diatomic lattice model representing the heterogeneous system is considered, and

* Corresponding author. Tel.: +1 765 494 6237.
E-mail address: hhhuang@purdue.edu (H.-H. Huang).

0020-7403/$ - see front matter © 2010 Elsevier Ltd. All rights reserved.
doi:10.1016/j.ijmecsci.2010.09.010

how the present multi-displacement continuum model captures the dynamic characteristics of the lattice system is studied.

2. First-order multi-displacement continuum model

A one-dimensional discrete system consisting of alternating masses m_1 and m_2 as shown in Fig. 1 is considered to illustrate the multi-displacement continuum concept. The pair-wise interactions between the adjacent periodic masses are represented by elastic springs with spring constants k_1 and k_2. The corresponding lattice spacing is denoted as L_1 and L_2. Because of the periodic characteristic of the lattice system, a unit cell enclosed by the dashed line, shown in Fig. 1, is considered to represent the overall responses of the discrete system. The dimension of the unit cell is L, equal to L_1+L_2. The displacements for the masses m_1 and m_2 are denoted as u_1 and u_2. It is noted that the displacements u_1 and u_2 are expressed in terms of the global coordinate system. Since the dimension of the unit cell is small as compared to the deformation gradient, the two displacement quantities are associated with the same material point in the continuum concept. As a result, the displacement fields in the (j)th unit cell are expressed explicitly as

$$u_1^{(j)} = u_1(x) \tag{1}$$

$$u_2^{(j)} = u_2(x) \tag{2}$$

When the length of the unit cell is sufficiently small as compared to the characteristic length of deformation, the displacement, $u_1^{(j+1)} = u_0$, at the right end of the unit cell can be approximated by the linear Taylor series expansion as

$$u_0(x) = u_1(x) + \frac{\partial u_1}{\partial x} L \tag{3}$$

The strain energy density, W, and kinetic energy density, T, in the unit cell are defined as the volume averages of the strain energy and kinetic energy of the unit cell, respectively. Assuming the volume of the unit cell to be $1 \times 1 \times L$ and using the relation of Eq. (3), one obtains

$$\begin{aligned} W &= \frac{1}{2L} k_1 (u_2 - u_1)^2 + \frac{1}{2L} k_2 (u_o - u_2)^2 \\ &= \frac{1}{2L} k_1 (u_2 - u_1)^2 + \frac{1}{2L} k_2 \left(u_1 + \frac{\partial u_1}{\partial x} L - u_2 \right)^2 \end{aligned} \tag{4}$$

and

$$T = \frac{1}{2L} m_1 (\dot{u}_1)^2 + \frac{1}{2L} m_2 (\dot{u}_2)^2 \tag{5}$$

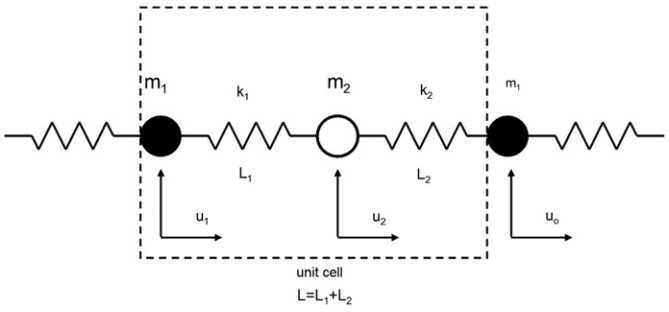

Fig. 1. One-dimensional discrete lattice model.

Expressions of W and T, shown above, can be regarded as the deformation and kinetic energy densities, respectively, at a point x in an equivalent one-dimensional continuum with two displacement vectors $u_1(x)$ and $u_2(x)$. By defining normal strain $\varepsilon = \partial u_1/\partial x$ and relative strain $\varepsilon_r = (u_2 - u_1)/L$, the deformation energy density function is rewritten as

$$W = \frac{Lk_1}{2} \varepsilon_r^2 + \frac{Lk_2}{2} (\varepsilon - \varepsilon_r)^2 \tag{6}$$

The constitutive relations for the equivalent continuum are then deduced as follows:

$$\sigma = \frac{\partial W}{\partial \varepsilon} = Lk_2 (\varepsilon - \varepsilon_r) \tag{7}$$

$$\sigma_r = \frac{\partial W}{\partial \varepsilon_r} = L(k_1 + k_2)\varepsilon_r - Lk_2 \varepsilon \tag{8}$$

where σ is the normal stress and σ_r is the relative stress.

By use of Hamilton's principle

$$\delta \int_{t_o}^{t_1} \int_V (T - W) dV\, dt + \int_{t_o}^{t_1} \int_S T_i \delta u_i dA\, dt = 0 \tag{9}$$

the equations of motion of the equivalent multi-displacement continuum are derived as

$$m_1 \ddot{u}_1 - (k_1 + k_2)u_2 + (k_1 + k_2)u_1 + k_2 L \frac{\partial u_2}{\partial x} - k_2 L^2 \frac{\partial^2 u_1}{\partial x^2} = 0 \tag{10}$$

$$m_2 \ddot{u}_2 - (k_1 + k_2)u_1 + (k_1 + k_2)u_2 - k_2 L \frac{\partial u_1}{\partial x} = 0 \tag{11}$$

together with the boundary condition

$$\tau = k_2 \left(u_1 - u_2 + \frac{\partial u_1}{\partial x} L \right) \tag{12}$$

in which τ is the applied boundary traction. It is noted that this boundary condition can be simplified by using constitutive relations Eqs. (7) and (8), and reduces to

$$\tau = k_2 (\varepsilon L - \varepsilon_r L) = Lk_2 (\varepsilon - \varepsilon_r) = \sigma \tag{13}$$

3. Static problem

In order to interpret the physical meanings of the normal and the relative strains defined earlier, we consider a uniform static deformation in the equivalent continuum, i.e. $\partial^2 u_1/\partial x^2 = 0$. Thus, u_1 assumes a linear form as

$$u_1 = Cx + D \tag{14}$$

In addition, from Eqs. (10) and (11), the following relation

$$\frac{\partial}{\partial x}(u_2 - u_1) = 0 \tag{15}$$

is obtained. Therefore, u_2 can be expressed as

$$u_2 = Cx + E \tag{16}$$

Substitution of Eqs. (14) and (16) into Eq. (11) leads to

$$(E - D) = \frac{k_2}{k_1 + k_2} LC \tag{17}$$

The coefficients, C, D and E in Eqs. (14) and (16), need to be determined from the boundary condition. From Eq. (12) in conjunction with (14) and (16), the coefficient C is expressed in

terms of the applied loading as

$$C=\frac{\tau}{L}\left(\frac{1}{k_1}+\frac{1}{k_2}\right) \tag{18}$$

Subsequently, from the definition of the normal strain, relative strain, relative stress and normal stress, the quantities are expressed alternatively in terms of the spring constants and the applied loading, τ, as

$$\varepsilon=\frac{\partial u_1}{\partial x}=\frac{\tau}{L}\left(\frac{1}{k_1}+\frac{1}{k_2}\right) \tag{19}$$

$$\varepsilon_r=\frac{u_2-u_1}{L}=\frac{E-D}{L}=\frac{\tau}{k_1L} \tag{20}$$

$$\sigma_r=L(k_1+k_2)\varepsilon_r-Lk_2\varepsilon=0 \tag{21}$$

$$\sigma=Lk_2(\varepsilon-\varepsilon_r)=\tau \tag{22}$$

It is evident from Eq. (19) that in the static case, normal strain ε represents the average strain generated in the unit cell of the original lattice, when subjected to a tensile loading. Also, the equivalent Young's modulus is $k_1k_2L/(k_1+k_2)$. The relative strain ε_r denotes the relative displacement of m_1 and m_2, divided by the total length of the unit cell. It is of interest to note that the re lative stress, σ_r, is equal to zero in the static simple loading case, while the normal stress, σ, is identical to the applied traction ,τ.

4. Harmonic wave propagation

We consider free harmonic wave propagation in the multi-displacement continuum medium. The displacement fields assume the form

$$u_1=A_1\exp[i(qx-\omega t)] \tag{23}$$

$$u_2=A_2\exp[i(qx-\omega t)] \tag{24}$$

where q is wavenumber, and ω is angular frequency. Substituting Eqs. (23) and (24) in equations of motion (10) and (11) yields two homogeneous equations for A_1 and A_2 as

$$\begin{bmatrix} -m_1\omega^2+(k_2q^2L^2+k_1+k_2) & -(k_1+k_2)+ik_2qL \\ -(k_1+k_2)-ik_2qL & -m_2\omega^2+(k_1+k_2) \end{bmatrix}\begin{Bmatrix} A_1 \\ A_2 \end{Bmatrix}=\begin{Bmatrix} 0 \\ 0 \end{Bmatrix} \tag{25}$$

The dispersion equation is obtained by solving the above eigen-value problem as

$$\omega^2=\frac{(m_1+m_2)(k_1+k_2)+m_2k_2(qL)^2}{2m_1m_2}\left(1\pm\sqrt{1-\frac{4m_1m_2k_1k_2(qL)^2}{[(m_1+m_2)(k_1+k_2)+m_2k_2(qL)^2]^2}}\right) \tag{26}$$

Two branches of wave form are obtained. The lower mode is the acoustic mode and the higher one is the optical mode. Fig. 2a and b shows, respectively, the dispersion curves for the acoustic and optical modes with the material constants chosen as $m_1=1$, $m_2=3$, $k_1=6$ and $k_2=1$. In addition, the dispersion curves obtained from the original one-dimensional lattice [9] are also included for comparison. It is evident that, for the acoustic mode, the dispersion curve predicted by the multi-displacement model agrees well with that of the lattice model for values of qL less than 2.5, which corresponds approximately to the wavelength $\lambda=2.5L$. For the optical mode, the multi-displacement solution is accurate for qL less than 0.5, i.e., $\lambda>12.6L$. When the wavenumber q approaches zero (long wavelength limit), the angular frequency of the optical mode reduces to

$$\omega=\left[\frac{(m_1+m_2)(k_1+k_2)}{m_1m_2}\right]^{1/2} \tag{27}$$

It should be noted that if the lattice is represented by a classical elastic solid (the effective modulus theory) with an effective Young's modulus derived based on the static consideration, then the wave motion is not dispersive and the optical mode is absent.

5. Discussion

5.1. Comparison of dispersion curves

Numerical results for the dispersion curves obtained with the first-order multi-displacement continuum and the effective modulus models are plotted in Fig. 3 for two different cases. Only the acoustic mode is shown because of the absence of the optical mode with the effective modulus model. Some aspects of interest are noted. First, the ratio of the lattice spacing L_1/L_2 does not affect the dispersion relation, since its effect is accounted for by spring constants. Second, it can be seen that, in both cases, the multi-displacement theory is more accurate than the effective modulus theory as the wavelength becomes shorter.

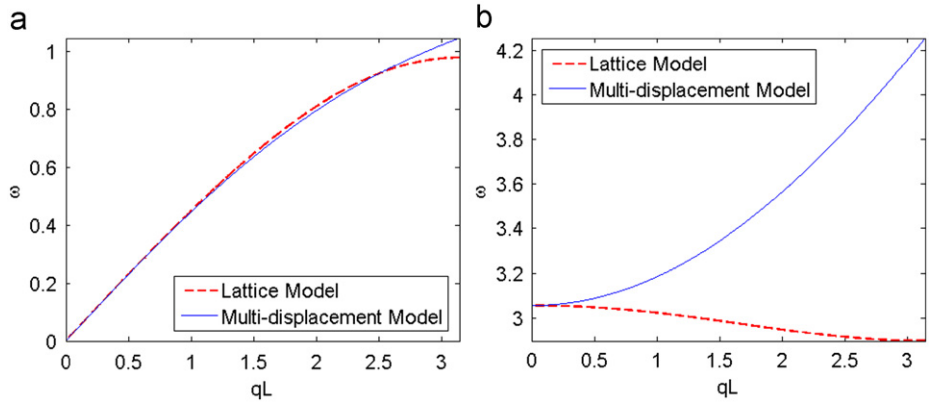

Fig. 2. Dispersion curves for the multi-displacement continuum model and the discrete lattice model in (a) acoustic mode and (b) optical mode.

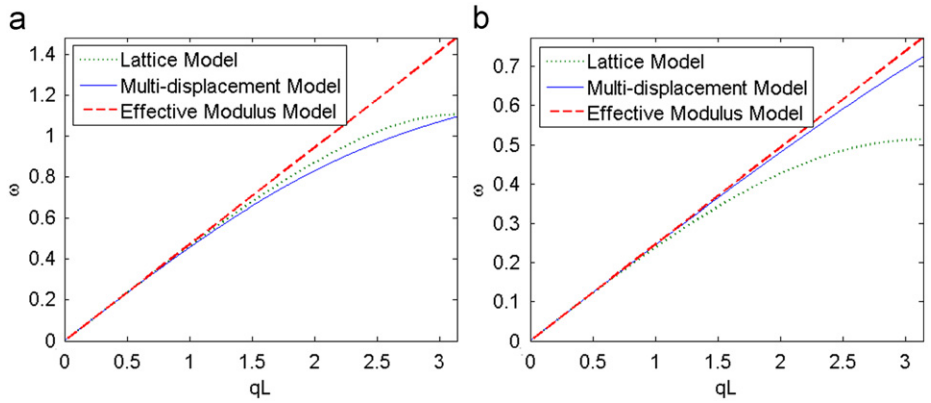

Fig. 3. Comparison of the dispersion curves for different models. Material constants are chosen as Case 1: $m_1=2$, $m_2=1$, $k_1=2$, $k_2=1$ and Case 2: $m_1=10$, $m_2=1$, $k_1=2$, $k_2=1$.

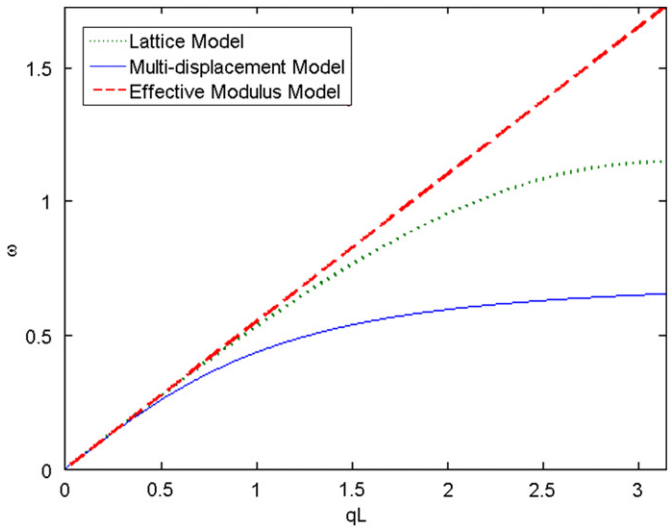

Fig. 4. The dispersion curves when the material constants are set $m_1=1$, $m_2=2$, $k_1=1$ and $k_2=10$.

5.2. Choice of unit cell

One can see from Fig. 3a that the multi-displacement model has over-corrected the dispersion curve from that of the original lattice model, i.e., frequencies predicted by the multi-displacement model are lower than those by the original lattice model within some range of wavenumbers. For the present case, the multi-displacement model represents the original lattice system pretty well. However, there are some cases for which the first-order multi-displacement model is not as accurate. Fig. 4 shows an example for the case $m_1=1$, $m_2=2$, $k_1=1$ and $k_2=10$. It is evident that the dispersion curve according to the first-order multi-displacement model deviates significantly from that of the original lattice model and the effective modulus model actually outperforms the multi-displacement model.

The reason for the poor representation is in part due to the choice of the unit cell. Recall that, in developing the multi-displacement model, the unit cell shown in Fig. 1 was selected. For cases where m_1/m_2 or k_1/k_2 is small, the two term series expansion for the displacement of mass 1 as given by the unit cell, as shown in Fig. 5, should be used. Note that the two mentioned unit cells actually form the same infinite lattice system. By adopting this alternative unit cell, we need not re-derive the earlier equations. The whole derivations are just slightly modified by interchanging notations 1 and 2. For instance, Eq. (3) is now

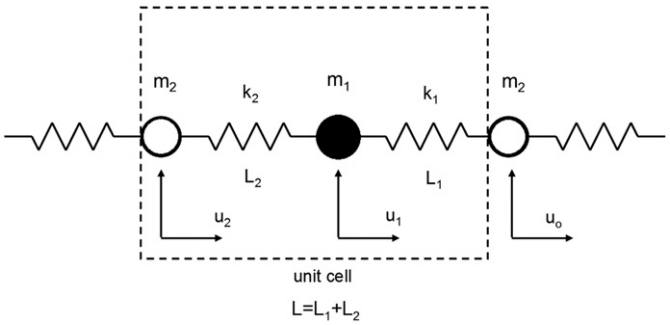

Fig. 5. Alternative unit cell to be chosen.

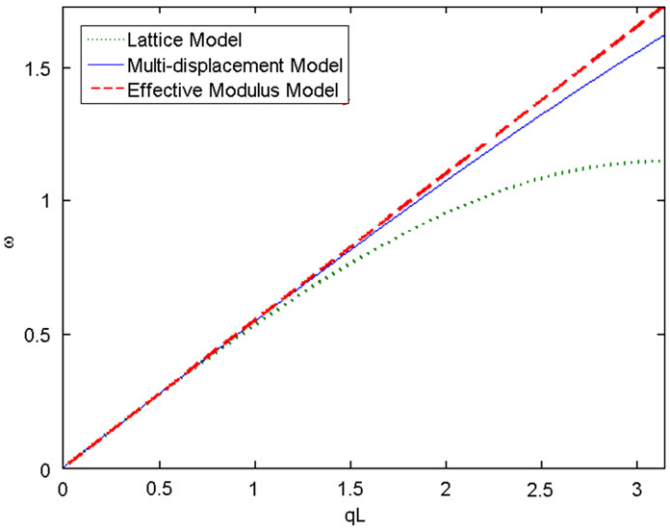

Fig. 6. Comparison of the dispersion curves for different models. Material constants are chosen as $m_1=1$, $m_2=2$, $k_1=1$ and $k_2=10$.

rewritten as

$$u_0(x)=u_2(x)+\frac{\partial u_2}{\partial x}L \tag{28}$$

In other words, the displacement of the denser or stiffer part of the unit cell is used for the series expansion. By using this approach, the dispersion curve for the case $m_1=1$, $m_2=2$, $k_1=1$ and $k_2=10$ is obtained and shown in Fig. 6. Much improved result is seen.

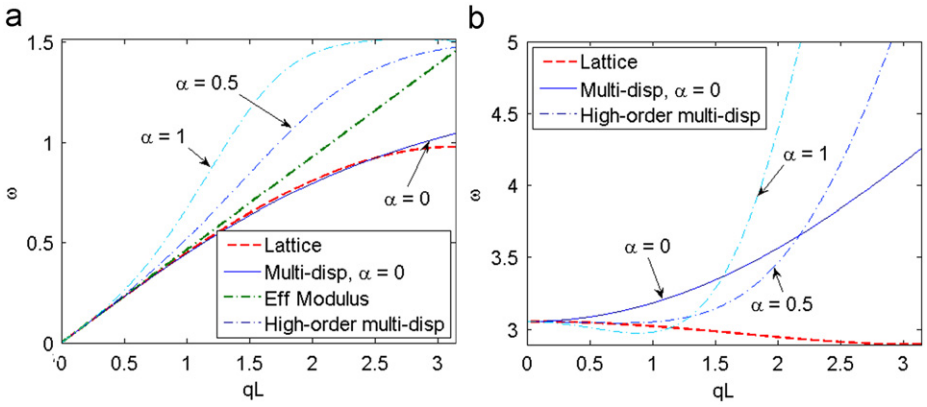

Fig. 7. Comparison of the dispersion curves for various α. Material constants are chosen as $m_1=1$, $m_2=3$, $k_1=6$ and $k_2=1$: (a) acoustic mode and (b) optical mode.

5.3. Higher order multi-displacement model

Another issue to be noted is that the optical mode cannot be well predicted by the present multi-displacement model (see Fig. 3b). In particular, the negative slope of the initial portion of the optical mode cannot be described by the first-order multi-displacement model. The negative slope of the dispersion curve indicates a negative group velocity, which has attracted attention from some researchers [15,16]. In order to capture the negative slope, we expand the displacement field of mass 1 by a higher-order Taylor series as

$$u_0(x)=u_1(x)+\frac{\partial u_1}{\partial x}L+\alpha\frac{\partial^2 u_1}{\partial x^2}L^2 \tag{29}$$

where α is a correction factor for truncation errors.

The strain energy density, W, and kinetic energy density, T, in the unit cell corresponding to the displacement expansion, given by Eq. (29) are, respectively

$$W=\frac{1}{2L}k_1(u_2-u_1)^2+\frac{1}{2L}k_2\left(u_1+\frac{\partial u_1}{\partial x}L+\alpha\frac{\partial^2 u_1}{\partial x^2}L^2-u_2\right)^2 \tag{30}$$

and

$$T=\frac{1}{2L}m_1(\dot{u}_1)^2+\frac{1}{2L}m_2(\dot{u}_2)^2 \tag{31}$$

According to Hamilton's principle, Eq. (9), the equations of motion of the higher order multi-displacement continuum are derived as

$$m_1\ddot{u}_1-k_1(u_2-u_1)+k_2(u_1-u_2)+(2\alpha-1)k_2L^2\frac{\partial^2 u_1}{\partial x^2}+\alpha^2k_2L^4\frac{\partial^4 u_1}{\partial x^4}+k_2L\frac{\partial u_2}{\partial x}-\alpha k_2L^2\frac{\partial^2 u_2}{\partial x^2}=0 \tag{32}$$

$$m_2\ddot{u}_2+k_1(u_2-u_1)-k_2(u_1-u_2)-k_2L\frac{\partial u_1}{\partial x}-\alpha k_2L^2\frac{\partial^2 u_1}{\partial x^2}=0 \tag{33}$$

It is seen that when $\alpha=0$, Eqs. (32) and (33) are identical to Eqs. (10) and (11). The dispersion relation can be obtained in a manner similar to that described in Section 4. Fig. 7 shows the dispersion curves obtained using the higher order multi-displacement model, with α varying from 0 to 1. For the acoustic mode, one sees that the dispersion curve with $\alpha=0$ best fits that of the lattice model. However, the advantage of introducing α can be seen from the dispersion curve of the optical mode, as shown in Fig. 7b. It is seen that, for a nonzero α, the optical mode of the dispersion curves starts to curve down at small wavenumbers (long wavelengths), and then curve up while the wavenumber increases. It is evident that curve of the higher order continuum model is in good agreement up to $qL=1$ with that of the lattice model when α is around 0.5. While improving the optical mode with $\alpha=0.5$, it actually causes the acoustic mode to deviate somewhat from the lattice solution.

6. Conclusion

Two multi-displacement microstructure continuum models are introduced to describe the dispersive behavior of a diatomic lattice model. The non-dispersive effective modulus model is employed for comparison. The first-order multi-displacement model, in general, describes the dispersion curve of the acoustic mode very well. However, it cannot describe the negative group velocity of the optical mode. The higher order continuum model is found able to describe the negative group velocity with the proper choice of a weighting factor for the higher order expansion term.

References

[1] Noor AK. Continuum modeling for repetitive lattice structures. Appl Mech Rev 1988;41:285–96.
[2] Lee U. Equivalent continuum models of large platelike lattice structures. Int J Solids Struct 1994;31:457–67.
[3] Kwon YW, Manthena C. Homogenization technique of discrete atoms into smeared continuum. Int J Mech Sci 2006;48:1352–9.
[4] Cosserat E, Cosserat F. Theorie des corps deformables. Paris: A. Hermann & Fils; 1909.
[5] Toupin RA. Elastic materials with couple-stresses. Arch Ration Mech Anal 1962;11:385–414.
[6] Mindlin RD. Micro-structure in linear elasticity. Arch Ration Mech Anal 1964;16:51–78.
[7] Eringen AC, Suhubi ES. Nonlinear theory of micro-elastic solids. Int J Eng Sci 1964;2:189–203.
[8] Sun CT, Achenbach JD, Herrmann G. Continuum theory for a laminated medium. ASME J Appl Mech 1968;35:467–75.
[9] Achenbach JD, Sun CT, Herrmann G. On the vibrations of a laminated body. ASME J Appl Mech 1968;35:689–96.
[10] Shibutani Y, Vitek V, Bassani JL. Nonlocal properties of inhomogeneous structures by linking approach of generalized continuum to atomistic model. Int J Mech Sci 1998;40:129–37.
[11] Chen YP, Lee JD. Connecting molecular dynamics to micromorphic theory. (I). Instantaneous and averaged mechanical variables. Physica A 2003;322:359–76.
[12] Sun CT, Huang GL. Modeling heterogeneous media with microstructures of different scales. J Appl Mech 2007;74:203–9.
[13] Huang GL, Sun CT. Continuum modeling of solids with micro/nanostructures. Philos Mag 2007;87:3689–707.
[14] Wang ZP, Sun CT. Modeling micro-inertia in heterogeneous materials under dynamic loading. Wave Motion 2002;36:473–85.
[15] McDonal KT. Negative group velocity. Am J Phys 2001;69:607–14.
[16] Dolling G, Enkrich C, Wegener M, Soukoulis CM, Linden S. Simultaneous negative phase and group velocity of light in a metamaterial. Science 2006;312:892–4.